The Cryosphere Discuss., doi:10.5194/tc-2016-21, 2016
Manuscript under review for journal The Cryosphere
Published: 2 February 2016

The Cryosphere Discussions
Open Access
EGU

Near Real Time Arctic sea ice thickness and volume from CryoSat-2

R. L. Tilling[1], A. Ridout, A. Shepherd[2]

[1] Centre for Polar Observation and Modelling, Department of Earth Sciences, University College London, London, WC1E 6BT, UK

[2] Centre for Polar Observation and Modelling, School of Earth and Environment, University of Leeds, Leeds, LS2 9JT, UK

Correspondence to: R. L. Tilling (rachel.tilling.12@ucl.ac.uk)

The Cryosphere Discuss., doi:10.5194/tc-2016-21, 2016
Manuscript under review for journal The Cryosphere
Published: 2 February 2016

Abstract. Timely observations of sea ice thickness help us to understand Arctic climate, and can support maritime activities in the Polar Regions. Although it is possible to calculate Arctic sea ice thickness using measurements acquired by CryoSat-2, the latency of the final release dataset is typically one month, due to the time required to determine precise satellite orbits. We use a new fast delivery CryoSat-2 dataset based on preliminary orbits to compute Arctic sea ice thickness in near real time (NRT), and analyse this data for one sea ice growth season from October 2014 to April 2015. We show that this NRT sea ice thickness product is of comparable accuracy to that produced using the final release CryoSat-2 data, with an average thickness difference of 5 cm, demonstrating that the satellite orbit is not a critical factor in determining sea ice freeboard. In addition, the CryoSat-2 fast delivery product also provides measurements of Arctic sea ice thickness within three days of acquisition by the satellite, and a measurement is delivered, on average, within 10, 7 and 6 km of each location in the Arctic every 2, 14 and 28 days respectively. The CryoSat-2 NRT sea ice thickness dataset provides an additional constraint for seasonal predictions of Arctic climate change, and will allow industries such as tourism and transport to navigate the polar oceans with safety and care.

1 Introduction

Arctic sea ice is a key component of the global climate system, and changes in its thickness and volume impact on regional heat (Sedlar et al., 2011) and freshwater (Aagaard and Carmack, 1989) budgets, and on subsequent patterns of atmospheric (Singarayer et al., 2006, Schweiger et al., 2008, Francis and Vavrus, 2012) and oceanic (Vellinga and Wood, 2002) circulation across the Arctic and at lower latitudes. The availability of Arctic-wide sea ice thickness data, especially in near real time (NRT), will enable evaluation and improved skill in the prediction of sea ice thickness distributions by climate models (Day et al., 2014) which, in turn, will benefit models of the global climate. In addition, there is increasing interest in the behaviour of Arctic sea ice among operational services, with a growing need for accurate and timely information of sea ice thickness. For example, shipping through the Arctic Ocean via the Northern Sea Route (NSR) could save about 40% of the sailing distance from Asia (Yokohama) to Europe (Rotterdam) compared to the traditional route via the Suez Canal (Liu and Kronbak, 2010), which would quicken the regional export of natural resources, and delivery of cargo to the communities along the Siberian coast (Meier et al., 2014). Ease of passage is also a concern for those looking to ship along the Northwest Passage and future trans-Arctic shipping routes along the Russian coast, and when considering the potential for tourism in regions such as Canadian Arctic waters (Stewart et al., 2007). The oil and gas sector require hemispheric studies of sea ice concentration, extent, motion and thickness (Galley et al., 2013) to estimate productions costs and to assess the feasibility and safety of replacing ice-based construction with lower cost conventional construction equipment (Harsem et al., 2011). As a consequence many large oil companies are reducing their plans for Arctic exploration and drilling activities due to the high costs and risks, which will impact on northern areas and communities through local businesses who report losses in hotel revenues, restaurant businesses, and the local marine support (Meier et al., 2014). Up-to-date measurements of sea ice thickness are crucial when considering building costs for exploration platforms and icebreaker ships, transit speeds, and navigation difficulties and risks. Here we present a method for obtaining NRT sea ice thickness measurements across the northern hemisphere using fast delivery CryoSat-2 data.

The Cryosphere Discuss., doi:10.5194/tc-2016-21, 2016
Manuscript under review for journal The Cryosphere
Published: 2 February 2016

A range of Arctic sea ice thickness measurements are currently available, with varying spatial and temporal coverage. The Beaufort Gyre Exploration Project (BGEP), based at the Woods Hole Oceanographic Institution in collaboration with researchers from Fisheries and Oceans Canada at the Institute of Ocean Sciences, have provided year-round sea ice draft data from upward looking sonar buoys since 2003, from three buoys in the Beaufort Sea. On a larger scale, NASA's Operation IceBridge utilises a suite of research aircraft each spring (March and April) to produce tracks of sea ice thickness estimates (Kurtz et al., 2013) concentrated around northern Greenland, the ocean region north of the Canadian Archipelago, and the Beaufort Sea. Currently the final and 'quick look' IceBridge data are available for spring 2009-2012 and spring 2013-2015, respectively. The quick look product is experimental and is designed only to be applicable for time-sensitive projects such as sea ice forecasting. On a larger spatial scale, there are currently three publically available datasets that provide sea ice thickness estimates across the whole Arctic Ocean. These datasets are produced by NASA (Kurtz et al., 2014), Germany's Alfred Wegener Institute (AWI) (Ricker et al., 2014), and the UK's Centre for Polar Observation and Modelling (CPOM) (Tilling et al., 2015) using final release data from the European Space Agency's (ESA) CryoSat-2 satellite (Wingham et al., 2006), which was launched in 2010. NASA provide monthly-averaged thickness data for March 2014 and March 2015 within a fixed central Arctic domain (Kwok et al., 2009). The NASA product is currently quick-look and experimental. AWI provide monthly averaged thickness data starting from January 2011 with a current lag of about 6 months, and these data again cover a central area of the Arctic Ocean. CPOM distribute sea ice thickness estimates for spring (March/April average) and autumn (October/November average) beginning in autumn 2010, also with a lag of about 6 months, depending on the availability of sea ice concentration data (Cavalieri et al., 1996, updated yearly). The CPOM estimates cover the entire northern hemisphere, defined as latitudes above and including 40° N.

2 Data and Methods

We use fast delivery radar altimeter measurements from the ESA CryoSat-2 satellite (Wingham et al., 2006) to produce NRT estimates of Northern Hemisphere (latitudes above 40° N) sea ice thickness and volume. The data are Level 1b, and consist of an echo for each point along the ground track of the satellite, which requires prior on-ground processing of the raw satellite data by ESA. Before March 26th 2015, ESA applied a processing chain known as 'Baseline-B' to the raw fast delivery data, and an updated processor, 'Baseline-C', has been applied since. The fast delivery CryoSat-2 data are available from ESA on average 36 hours after acquisition by the satellite, although we run our sea ice processor with a latency of three days to ensure sufficient data are available. The main difference between the fast delivery and final release CryoSat-2 data is the orbits applied. For both datasets, an accurate determination of the satellite orbit is required to determine surface elevations above a reference ellipsoid. For the final release data product, ESA perform a ground-based Precise Orbit Determination (POD), which requires modelling of the forces acting on the satellite as well as a dense set of measurements regarding its position and velocity (Wingham et al., 2006). The primary means of making these measurements is with the on-board Doppler Orbit and Radio positioning Integration by Satellite (DORIS) receiver, which makes measurements of the relative velocity of the satellite to an extensive network of ground beacons. The messages uplinked from the beacons include time signals that allow the DORIS receiver time to be accurately determined. The DORIS receiver also includes software for the real-time, on-board computation of the orbit, known as the DORIS

The Cryosphere Discuss., doi:10.5194/tc-2016-21, 2016
Manuscript under review for journal The Cryosphere
Published: 2 February 2016

Navigator orbit. The DORIS Navigator orbit is estimated to be accurate to 30 cm in the radial direction, and is included in the fast delivery CryoSat-2 data to provide good quality orbit estimates before the POD can be produced. However, the fast delivery data are more susceptible to orbit dropout, meaning that certain orbits, for which the orientation of the satellite could not be sufficiently determined, are not included in the dataset. Geophysical corrections are often missing in the fast delivery data. On average, it takes six hours to process one day of data.

The first processing step (Tilling et al., 2015) is the computation of sea ice freeboard, which is the difference in elevation between the snow-ice interface and that of the surrounding ocean. We do this by using the return echo shape to discriminate between measurements of the ocean surface and the ice surface (Peacock and Laxon, 2004). We define sea ice regions as those with a NRT sea ice concentration (Maslanik and Stroeve, 1999, updated daily) greater than 75%. NRT ice concentration data are taken from the National Snow and Ice Data Center (NSIDC) and are available to us by 01:00 UTC two days after measurement. Sea ice thickness is then calculated from freeboard measurements, by assuming that the ice floats in hydrostatic equilibrium and using estimates of snow depth and density derived from a climatology (Warren et al., 1999), fixed estimates of first-year ice (FYI) and multi-year ice (MYI) densities (Alexandrov et al., 2010), a fixed seawater density (Wadhams et al., 1992), and a reduced fraction of snow on FYI (Kurtz and Farrell, 2011). NRT ice type data from the Norwegian Meteorological Service Ocean and Sea Ice Satellite Application Facility (http://osisaf.met.no/p/ice/#type) are used to classify FYI and MYI for each individual freeboard measurement, and this dataset is available to us by 01:00 UTC the day after measurement. During the sea ice melt season it becomes difficult to discriminate between measurements of the ocean and the ice due to melt ponds that form on the sea ice surface, and because of this we do not currently produce measurements of sea ice thickness between May and September. NRT sea ice thickness data are output Arctic-wide on a 5 km square grid (Fig. 1), or for user-configurable regions of interest (ROI) on a 1 km square grid. To obtain Arctic-wide and ROI grid values, a circular operator is applied to all thickness measurements within a 25 and 5 km radius of the centre of the grid, respectively, with all points receiving equal weighting. We then compute sea ice volume Arctic-wide and within fixed oceanographic basins (Nurser and Bacon, 2014, Tilling et al., 2015) by averaging individual thickness and concentration values during each calendar month on a 0.1 by 0.5 degree grid, and defining the sea ice margin by applying a 15% sea ice concentration mask using data from the 15th day of each month. Empty grid points within the sea ice extent mask are filled by nearest neighbour interpolation. Monthly estimates of sea ice volume are then calculated by summing the product of the ice thickness, the ice concentration, and the ice area, within the sea ice extent mask.

We estimate monthly errors in NRT Arctic-wide sea ice volume and mean thickness (Tilling et al., 2015) by considering the contributions due to uncertainties in snow depth (4.0 to 6.2 cm) (Warren et al., 1999), snow density (60.0 to 81.6 kg m^{-3}) (Warren et al., 1999), sea ice density (7.6 kg m^{-3}) (Romanov, 2004, Tilling et al., 2015), sea ice concentration (5%), and sea ice extent (20,000 to 30,000 km^2) (http://nsidc.org/arcticseaicenews/faq/#error_bars). Although individual freeboard measurements have a standard deviation of about 9 cm Arctic-wide, we typically include more than 1 million observations in each estimate of monthly volume, and so the impact of this variability is negligible on the volume uncertainty. Uncertainties in seawater density also have a negligible impact on the uncertainty in volume (Kurtz et al., 2013, Ricker et al., 2014). For NRT volume uncertainties, we compute the monthly rate of change of volume with respect to each parameter that has an associated error. We do this by individually

The Cryosphere Discuss., doi:10.5194/tc-2016-21, 2016
Manuscript under review for journal The Cryosphere
Published: 2 February 2016

adjusting the value for each parameter six times, at even increments, and re-computing the volume each time. The computed rates of change are then multiplied by the error in each parameter in question to estimate their partial contributions to the total volume error. Finally, we combine the monthly contribution to the volume error for all significant error sources in a root-sum-square manner to arrive at an estimate of the total monthly sea ice volume error. We estimate that year-to-year uncertainties in Arctic-wide sea ice volume are typically about 13.5%, with small variations from month to month (Tilling et al., 2015).

To estimate errors in sea ice thickness at smaller length scales, we consider the manner in which its contributions de-correlate in space. The major factors in the sea ice volume error budget are uncertainties in snow depth, snow density, and in sea ice density, each quantified as the standard deviation of monthly-averaged sparse field observations. These factors, and their variability, are influenced by synoptic-scale meteorology, and we estimate that the largest length scale over which they are correlated is comparable to that of a typical polar vortex, around 2000 km in diameter (http://www.cpc.ncep.noaa.gov/products/stratosphere/polar/polar.shtml). This corresponds to a region similar in size to the Eurasian Basin (Nurser and Bacon, 2014, Tilling et al., 2015), or 35% of the central Arctic; the region within which field observations of snow depth, snow density, and sea ice density were made. Based on this assumption we estimate that Arctic-wide, errors in sea ice volume and thickness are reduced to 1/N^0.5 of their value at smaller scales as a consequence of being averaged over a greater area, where N is the ratio of the central Arctic area (9 million km^2) to that of the smaller region. We therefore estimate that the uncertainty of sea ice thickness is 23% for any measurement on our Arctic-wide, 5 km grid. However, we note that this is likely to be an overestimate, owing to the sparse sampling of the field observations used to obtain the uncertainties in its constitution (Warren et al., 1999). Although the variability of individual sea ice thickness measurements also contribute towards the uncertainty of the grid product, these measurements are averaged in sufficiently large numbers by the 25 km circular operator we employ to make this source of uncertainty negligible.

To assess the reliability of our NRT sea ice thickness and volume estimates, we compared them to our archive products derived from the final CryoSat-2 data release, which have shown excellent agreement with an extensive set of independent observations (Tilling et al., 2015). It is currently not possible to evaluate our NRT sea ice product against *in situ* measurements, as the overlap between coverage periods is too short. The comparison was done using seven months of data acquired between October 2014 and April 2015, which corresponds to a season of ice growth. The archive thickness data use final sea ice concentration from NSIDC (Cavalieri et al., 1996, updated yearly), rather than the NRT concentration data used in our NRT thickness and volume calculations. There is also a difference in the timeframe of on-ground processing of the raw data by ESA. Before February 22nd 2015, ESA applied the 'Baseline-B' processing chain to the raw final release data, and an updated processor, 'Baseline-C', has been applied since April 1st 2015. Between these dates, a hybrid processor known as 'Baseline-BC' was applied. In general, our NRT and archive estimates of sea ice thickness and volume are in excellent agreement, with an average difference of 5 cm and 175 km^3, respectively (Fig. 2a). These differences are well within the corresponding estimates of NRT and archive (Tilling et al., 2015) sea ice thickness and volume uncertainties. The archive estimates of sea ice volume are larger in part as a consequence of using the final sea ice concentration data set, which contains higher values than its NRT counterpart. For example, we recalculated sea ice volume using the NRT sea ice thickness and final sea ice concentration data sets, and the departure from the archive

The Cryosphere Discuss., doi:10.5194/tc-2016-21, 2016
Manuscript under review for journal The Cryosphere
Published: 2 February 2016

estimate reduced to 100 km^3. The remaining difference is likely due to the absence f certain orbits of CryoSat-2 data in the fast delivery product, rather than the difference in accuracy of the orbits or geophysical corrections applied to each product release, because most orbital and geophysical signals will be removed when differencing the sea ice and ocean surface elevations to calculate sea ice freeboard. We conclude, therefore, that the satellite orbits applied to fast delivery CryoSat-2 data are sufficient to determine accurate measurements of Arctic sea ice thickness and volume.

3 Results

The spatial distribution of the NRT sea ice thickness data (Fig. 1) for any given time period depends on the nature of the CryoSat-2 orbit over that period. CryoSat-2 has an orbit repeat period of 369 days, which is built up by successive shifts of a 30-day repeat sub-cycle, meaning that uniform coverage of the Arctic Ocean is achieved every 30 days (Wingham et al., 2006). The density of orbit crossovers increases with latitude up to the CryoSat-2 limit of 88°N, and also with the number of days of coverage. We produce Arctic-wide maps of NRT sea ice thickness for the previous 2, 14, and 28 day periods. CryoSat-2 orbit patterns are visible in maps of thickness for the final 2 (e.g. Fig. 1a and Fig. 1d) and 14 (e.g. Fig. 1b and Fig. 1e) days of each month. The orbits are clearer at lower latitudes, below about 80°N. Over 28 days, almost complete coverage across the sea ice pack is achieved. However, there are still small areas of unmapped sea ice, and these typically occur at the ice edge (see Fig. 1). In these unmapped areas the sea ice concentration is above 15%, which we use as the sea ice margin threshold, but below 75%, which is the concentration required for a region to be classed as containing sea ice (see Data and Methods).

To determine the utility of the 5 km grid measurements of NRT sea ice thickness for operational use, we performed a detailed assessment of the spatial and temporal distribution of the data. Over the 2, 14 and 28 day time periods for which it is available, we calculated the percentage of sea ice covered by the data in 1 degree latitude bands from 60-90°N, for the final 2, 14 and 28 days of each month. This was done for data from October 2014 to April 2015, and averaged over all months (Fig. 3a). We produced the equivalent plot for the mean data separation in each latitude band, where separation is simply the square root of the number of measurements in each band, divided by the sea ice covered area (Fig. 3b). For 28 days data coverage, sea ice at latitudes between 85-88°N is mapped in its entirety by the NRT product and the data separation drops to 5.0 km in each 1 degree latitude band, which is simply the grid separation. For 14 days coverage the CryoSat-2 orbit pattern achieves its maximum coverage, of 98%, between 86 and 87°N, which corresponds to a mean data separation of 5.1 km. The maximum coverage over 2 days is 91%, between 87 and 88°N, where the mean data separation is 5.2 km. The percentage of ice mapped decreases with decreasing latitudes, and the separation between data points increases, although there is some fluctuation in these trends that is likely due orbit dropout, or the shift in the CryoSat-2 orbit pattern producing less favourable coverage for a given month. CryoSat-2 does not observe sea ice north of 88°N, so the percentage of ice mapped drops to 0% for 2, 14 and 28 days coverage in the region 88-90°N. On average, the NRT sea ice thickness data maps 20, 57 and 74% of the Arctic sea ice north of 60°N every 2, 14 and 28 days respectively. This corresponds to a measurement within 10, 7 and 6 km of each location in the Arctic every 2, 14 and 28 days.

The Cryosphere Discuss., doi:10.5194/tc-2016-21, 2016
Manuscript under review for journal The Cryosphere
Published: 2 February 2016

The distribution of our NRT sea ice thickness measurements also varies with oceanographic basin and month, and the nature of the monthly variation depends on the region being observed. This is an important consideration for those wishing to use the data in a specific region of interest, or over the entirety of the sea ice growth season. We calculated the percentage of ice cover mapped by our NRT product for six key oceanographic basins (Fig. 4a), for the final 28 days of each month of the 2014-2015 sea ice growth season (Fig. 4b). The percentage of the ice cover mapped in the Amerasian and Eurasian basins is high (≥ 76%), with just a small increase over the growth season. Both regions are almost entirely covered in sea ice year-round, which means that the areal fraction of unmapped sea ice at the ice edge (see Fig. 1) is fairly consistent throughout the year. However, this is not the case for regions with more seasonal ice cover, such as the Canadian Archipelago and Northwest Passage, Hudson Bay, and the Beaufort Sea, where coverage improves throughout the growth season and peaks in February or March. In these regions, as the extent of the sea ice cover increases through winter, the unmapped area at the sea ice edge becomes a decreasing fraction of the ice-covered area, and a greater percentage of the ice cover is mapped. In addition, as the sea ice concentration increases through winter, echoes from sea ice floes becomes less noisy and are more likely to be included in our processing. Coverage in the Greenland Sea generally improves throughout the growth season, although there is some variation in this pattern due to fluctuations in the width of the unmapped area at the sea ice edge, which could be a consequence of the rapid sea ice transport in this sector. Overall, coverage is lowest for the Greenland Sea, Canadian Archipelago and Northwest Passage, and Hudson Bay. Due to the location of the Greenland Sea, there is also a persistent presence of unmapped sea ice along its eastern edge. The Canadian Archipelago and Northwest Passage, and Hudson Bay are in close proximity to substantial coastal areas, where it is difficult to construct sea surface height due to the absence of leads in the sea ice pack.

We extended our analysis of NRT data sampling by calculating the percentage of sea ice mapped in all Arctic Ocean basins at the beginning and end of the sea ice growth season (Table 1). For this calculation, we considered the percentage of ice cover mapped in the final 2, 14 and 28 days of each month. In each month the coverage improves with the number of days sampling, in every basin. The coverage also improves from October to March, for each time period, for all but one basin; the Canadian Archipelago/Northwest Passage experiences a drop in coverage over the growth season, for the 2-day observation period. However, this change is very small, and over short observation periods we would expect some variability in the proportion of ice cover mapped as a consequence of the CryoSat-2 orbital repeat pattern. This becomes more important in regions such as the Canadian Archipelago, where there is a high fraction of land interspersed with ocean. The Bering Sea, the Sea of Okhotsk, the White Sea, the Baltic Sea and surrounding Gulfs and the Labrador Sea have the smallest proportional ice cover mapped in March 2015. These are regions of highly seasonal sea ice cover, and by the end of the growth season the unmapped area at the ice edge still constitutes a sizable fraction of the ice–covered area. In addition, they are all southerly basins (below 70°N), which are sampled with reduced spatial density by CroSat-2. The most extensively sampled areas are in the central Arctic - the Amerasian and Eurasian basins - which experience substantial year-round sea ice cover and are at high latitudes. We conclude that the location, seasonality, and dynamic nature of any sea ice region are important considerations when assessing the reliability of the NRT Arctic sea ice thickness product.

The Cryosphere Discuss., doi:10.5194/tc-2016-21, 2016
Manuscript under review for journal The Cryosphere
Published: 2 February 2016

4 Discussion and Conclusions

Our CryoSat-2 NRT sea ice thickness dataset will benefit Arctic sea ice projections, because it can be used to constrain physical models that investigate the sensitivity of the region to climate change (Day et al., 2014) in a timely manner. It will also assist Arctic operations that rely on accurate and timely information on sea ice thickness, such as natural resource exploration (Galley et al., 2013), and shipping for cargo (Liu and Kronbak, 2010) and tourism (Stewart et al., 2007). A previous study (Rinne and Similä, 2016) has highlighted the potential value of fast delivery CryoSat-2 data for the classification of sea ice into discrete stages of its development – thin (<70 cm) and thick (>70 cm) FYI and MYI – in the Kara Sea. Our product extends this analysis to provide continuous measurements of sea ice thickness across the entire northern hemisphere, complementing established records of sea ice concentration (Cavalieri et al., 1996, updated yearly, Maslanik and Stroeve, 1999, updated daily) upon which annual assessments (Stroeve et al., 2005) and forecasts (Posey et al., 2011) of Arctic conditions are based. Timely availability of sea ice concentration estimates (Maslanik and Stroeve, 1999, updated daily) and sea ice type classifications (http://osisaf.met.no/p/ice/#type) are crucial for the rapid computation of our NRT sea ice thickness measurements. The NSIDC sea ice concentration and OSISAF sea ice type data are available to us by 01:00 UTC two days after, and 01:00 UTC the day after measurement, respectively. The fast delivery CryoSat-2 data are typically available 36 hours after acquisition from the satellite, but can vary from 1-3 days, so we run our sea ice processor at a latency of three days to ensure sufficient data is available. Processing one day of data for the northern hemisphere takes six hours, on average. A more rapidly delivered product would require the CryoSat-2 data to be consistently available within 36 hours, and sea ice concentration data to become available sooner, or that older concentration measurements were used as an approximation.

By using a new fast delivery CryoSat-2 dataset we are able to produce estimates of sea ice thickness across the northern hemisphere three days after acquisition from the satellite. This marks the beginning of a new phase for the CryoSat-2 mission, in which its primary data can be used for operational purposes. The NRT estimates are of comparable accuracy to those produced using the final release CryoSat-2 data, with an average difference of 5 cm between NRT and archive estimates of sea ice thickness. For the period from October 2014 to April 2015, the NRT dataset covers an average of 20, 57 and 74% of the Arctic sea ice north of 60°N every 2, 14 and 28 days respectively. This is equivalent to a measurement within 10, 7 and 6 km of each location in the Arctic every 2, 14 and 28 days. However, there are temporal and spatial variations in the data coverage. The time of year, location, and dynamic nature of any region of interest must be considered when assessing the reliability of the data. The next steps in the advancement of the data are to develop improved estimates of snow loading on Arctic sea ice, and to encourage users to utilise the data for model assessments and to constraint the physics of sea ice within models that form the basis of future climate projections.

Author contribution

R. L. Tilling and A. Ridout developed and analysed the satellite observations. A. Shepherd supervised the work. R. L. Tilling, A. Ridout and A. Shepherd wrote the paper. All authors commented on the text.

The Cryosphere Discuss., doi:10.5194/tc-2016-21, 2016
Manuscript under review for journal The Cryosphere
Published: 2 February 2016

Acknowledgements

Our NRT sea ice thickness data are publically available at http://www.cpom.ucl.ac.uk/csopr/seaice.html. We wish to thank those who provide the timely ancillary data that we require to deliver a NRT product: ESA, for the fast delivery CryoSat-2 Level 1B radar altimeter data (available via ftp at ftp://science-pds.cryosat.esa.int); OSI SAF, for their sea ice type maps (http://osisaf.met.no/p/ice/#type); and NSIDC, for NRT DMSP SSMIS Daily Polar Gridded Sea Ice Concentrations (available via ftp at ftp://sidads.colorado.edu/pub/DATASETS/nsidc0081_nrt_nasateam_seaice). This work was funded by the UK Natural Environment Research Council, with support from the UK National Centre for Earth Observation.

References

Aagaard, K. and Carmack, E. C. (1989) 'The role of sea ice and other fresh-water in the Arctic circulation', *Journal of Geophysical Research-Oceans,* 94(C10), pp. 14485-14498.

Alexandrov, V., Sandven, S., Wahlin, J. and Johannessen, O. M. (2010) 'The relation between sea ice thickness and freeboard in the Arctic', *The Cryosphere,* 4, pp. 373-380.

Cavalieri, D. J., Parkinson, C. L., Gloersen, P. and Zwally, H. J. (1996, updated yearly) 'Sea Ice Concentrations from Nimbus-7 SMMR and DMSP SSM/I-SSMIS Passive Microwave Data [concentration]. '.

Day, J. J., Tietsche, S. and Hawkins, E. (2014) 'Pan-Arctic and Regional Sea Ice Predictability: Initialization Month Dependence', *Journal of Climate,* 27(12), pp. 4371-4390.

Francis, J. and Vavrus, S. (2012) 'Evidence linking Arctic amplification to extreme weather in mid-latitudes', *Geophysical Research Letters,* 39(6), pp. L06801-1 - L06801-6.

Galley, R. J., Else, B. G. T., Prinsenberg, S. J., Babb, D. and Barber, D. G. (2013) 'Summer Sea Ice Concentration, Motion, and Thickness Near Areas of Proposed Offshore Oil and Gas Development in the Canadian Beaufort Sea — 2009', *Arctic,* 66(1), pp. 105-116.

Harsem, O., Eide, A. and Heen, K. (2011) 'Factors influencing future oil and gas prospects in the Arctic', *Energy Policy,* 39(12), pp. 8037-8045.

Kurtz, N. T. and Farrell, S. L. (2011) 'Large-scale surveys of snow depth on Arctic sea ice from Operation IceBridge', *Geophysical Research Letters,* 38(20), pp. L20505-1 - L20505-5.

Kurtz, N. T., Farrell, S. L., Studinger, M., Galin, N., Harbeck, J. P., Lindsay, R., Onana, V. D., Panzer, B. and Sonntag, J. G. (2013) 'Sea ice thickness, freeboard, and snow depth products from Operation IceBridge airborne data', *The Cryosphere,* 7(4), pp. 1035-1056.

The Cryosphere Discuss., doi:10.5194/tc-2016-21, 2016
Manuscript under review for journal The Cryosphere
Published: 2 February 2016

Kurtz, N. T., Galin, N. and Studinger, M. (2014) 'An improved CryoSat-2 sea ice freeboard retrieval algorithm through the use of waveform fitting', *The Cryosphere,* 8, pp. 1217-1237.

Kwok, R., Cunningham, G. F., Wensnahan, M., Rigor, I., Zwally, H. J. and Yi, D. (2009) 'Thinning and volume loss of the Arctic Ocean sea ice cover: 2003-2008', *Journal of Geophysical Research-Oceans,* 114(C7), pp. C07005-1 - C07005-16.

Liu, M. and Kronbak, J. (2010) 'The potential economic viability of using the Northern Sea Route (NSR) as an alternative route between Asia and Europe', *Journal of Transport Geography,* 18(3), pp. 434-444.

Maslanik, J. and Stroeve, J. C. (1999, updated daily) 'Near-Real-Time DMSP SSM/I-SSMIS Daily Polar Gridded Sea Ice Concentrations [concentration]'.

Meier, W. N., Hovelsrud, G. K., van Oort, B. E. H., Key, J. R., Kovacs, K. M., Michel, C., Haas, C., Granskog, M. A., Gerland, S., Perovich, D. K., Makshtas, A. and Reist, J. D. (2014) 'Arctic sea ice in transformation: A review of recent observed changes and impacts on biology and human activity', *Reviews of Geophysics,* 52(3), pp. 185-217.

Nurser, A. J. G. and Bacon, S. (2014) 'The Rossby radius in the Arctic Ocean', *Ocean Science* 10, pp. 967-975.

Peacock, N. R. and Laxon, S. W. (2004) 'Sea surface height determination in the Arctic Ocean from ERS altimetry', *Journal of Geophysical Research-Oceans,* 109(C7), pp. C07001-1 - C07001-14.

Posey, P. G., Hebert, D. A., Metzger, E. J., Wallcraft, A. J., Cummings, J. A., Preller, R. H., Smedstad, O. M. and Phelps, M. W. (2011) 'Real-time Data Assimilation of satellite derived ice concentration into the Arctic Cap Nowcast/Forecast System (ACNFS) ', *Oceans 2011*, pp. 1-4.

Ricker, R., Hendricks, S., Helm, V., Skourup, H. and Davidson, M. (2014) 'Sensitivity of CryoSat-2 Arctic sea-ice freeboard and thickness on radar-waveform interpretation', *The Cryosphere,* 8(4), pp. 1607-1622.

Rinne, E. and Similä, M. (2016) 'Utilisation of CryoSat-2 SAR altimeter in operational ice charting', *The Cryosphere* 10, pp. 121-131.

Romanov, I. P. (2004) 'Morphometric Characteristics of Ice and Snow in the Arctic Basin: Aircraft Landing Observations from the Former Soviet Union, 1928-1989'.

Schweiger, A., Lindsay, R. W., Vavrus, S. and Francis, J. A. (2008) 'Relationships between Arctic sea ice and clouds during autumn', *Journal of Climate,* 21(18), pp. 4799-4810.

Sedlar, J., Tjernstrom, M., Mauritsen, T., Shupe, M. D., Brooks, I. M., Persson, P. O. G., Birch, C. E., Leck, C., Sirevaag, A. and Nicolaus, M. (2011) 'A transitioning Arctic surface energy budget: the impacts of solar zenith angle, surface albedo and cloud radiative forcing', *Climate Dynamics,* 37(7-8), pp. 1643-1660.

Singarayer, J. S., Bamber, J. L. and Valdes, P. J. (2006) 'Twenty-first-century climate impacts from a declining Arctic sea ice cover', *Journal of Climate,* 19(7), pp. 1109-1125.

The Cryosphere Discuss., doi:10.5194/tc-2016-21, 2016
Manuscript under review for journal The Cryosphere
Published: 2 February 2016

Stewart, E. J., Howell, S. E. L., Draper, D., Yackel, J. and Tivy, A. (2007) 'Sea ice in Canada's Arctic: Implications for cruise tourism', *Arctic,* 60(4), pp. 370-380.

Stroeve, J. C., Serreze, M. C., Fetterer, F., Arbetter, T., Meier, W., Maslanik, J. and Knowles, K. (2005) 'Tracking the Arctic's shrinking ice cover: Another extreme September minimum in 2004', *Geophysical Research Letters,* 32(4).

Tilling, R. L., Ridout, A., Shepherd, A. and Wingham, D. J. (2015) 'Increased Arctic sea ice volume after anomalously low melting in 2013', *Nature Geoscience,* 8, pp. 643-646.

Vellinga, M. and Wood, R. A. (2002) 'Global climatic impacts of a collapse of the Atlantic thermohaline circulation', *Climatic Change,* 54(3), pp. 251-267.

Wadhams, P., Tucker, W. B. I., Krabill, W. B., Swift, J. C., Comiso, J. C. and Davis, N. R. (1992) 'Relationship between sea ice freeboard and draft in the Arctic Basin, and implications for ice thickness monitoring', *Journal of Geophysical Research-Oceans,* 97(C12), pp. 20325–20334.

Warren, S. G., Rigor, I. G., Untersteiner, N., Radionov, V. F., Bryazgin, N. N., Aleksandrov, Y. I. and Colony, R. (1999) 'Snow depth on Arctic sea ice', *Journal of Climate,* 12(6), pp. 1814-1829.

Wingham, D. J., Francis, C. R., Baker, S., Bouzinac, C., Brockley, D., Cullen, R., de Chateau-Thierry, P., Laxon, S. W., Mallow, U., Mavrocordatos, C., Phalippou, L., Ratier, G., Rey, L., Rostan, F., Viau, P. and Wallis, D. W. (2006) 'CryoSat: A mission to determine the fluctuations in Earth's land and marine ice fields', in Singh, R.P. & Shea, M.A. (eds.) *Natural Hazards and Oceanographic Processes from Satellite Data: Vol. 4 Advances in Space Research-Series*, pp. 841-871.

The Cryosphere Discuss., doi:10.5194/tc-2016-21, 2016
Manuscript under review for journal The Cryosphere
Published: 2 February 2016

Table 1: Variations in the sampling of CryoSat-2 near real time (NRT) sea ice thickness products in 17 Arctic Ocean basins. Regions 1-10 encompass all October sea ice, and regions 1-16 encompass all March sea ice. Region 17 is a sub-region of region 1 (Figure 4a).

	Data Coverage (% of ice cover mapped)					
	2 days		14 days		28 days	
	Oct 2014	Mar 2015	Oct 2014	Mar 2015	Oct 2014	Mar 2015
Amerasian Basin (1)	33	38	78	82	92	98
Eurasian Basin (2)	24	44	58	73	76	88
Canadian Archipelago & Northwest Passage (3)	9	7	31	37	39	53
Hudson Bay (4)	0	6	0	48	0	71
Baffin Bay (5)	0	15	0	56	0	81
Greenland Sea (6)	8	13	31	50	49	63
Iceland Sea (7)	0	16	0	44	0	57
Barents Sea (8)	0	9	17	32	18	47
Kara Sea (9)	2	17	15	46	16	58
Siberian Shelf Seas (10)	11	20	38	60	49	85
Bering Sea (11)	n/a	3	n/a	35	n/a	40
Sea of Okhotsk (12)	n/a	0	n/a	21	n/a	33
White Sea (13)	n/a	0	n/a	6	n/a	6
Baltic Sea & surrounding Gulfs (14)	n/a	0	n/a	0	n/a	0
Labrador Sea (15)	n/a	1	n/a	13	n/a	19
Gulf of St Laurence & Nova Scotia Peninsula (16)	n/a	n/a	n/a	n/a	n/a	n/a
Beaufort Sea (17)	17	20	59	83	69	95

The Cryosphere Discuss., doi:10.5194/tc-2016-21, 2016
Manuscript under review for journal The Cryosphere
Published: 2 February 2016

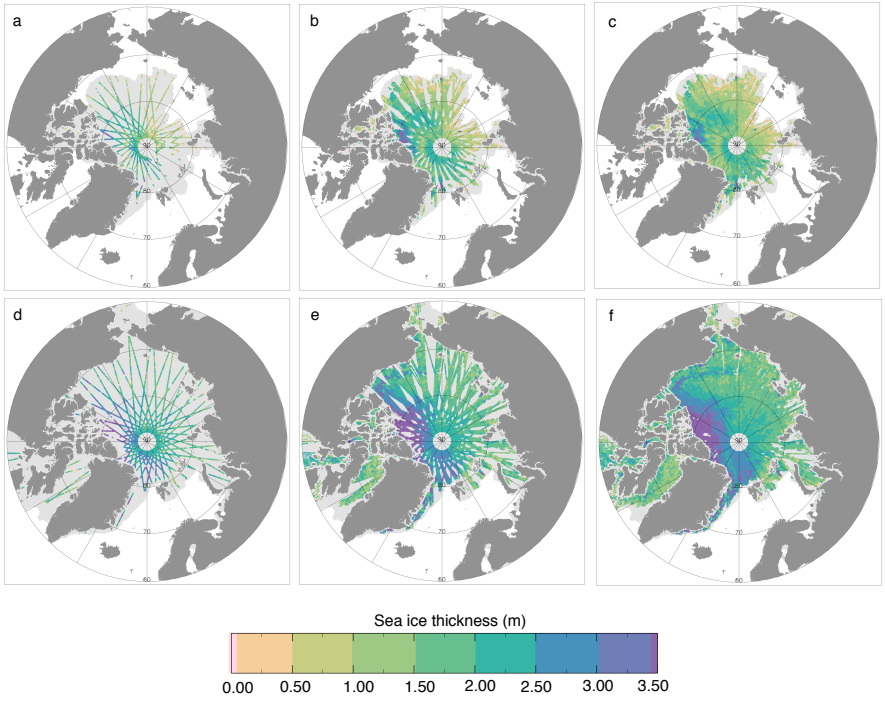

Figure 1: Near real time (NRT) Arctic sea ice thickness estimates from CryoSat-2. (a)-(c) Thickness estimates for the final 2, 14 and 28 days in October 2014, respectively. (d)-(f) Thickness estimates for the final 2, 14 and 28 days in March 2015, respectively. NRT sea ice thickness data are output Arctic-wide on a 5 km square grid. A circular operator is applied to all thickness measurements within a 25 km radius of the centre of the grid, with all points receiving equal weight. The sea ice extent mask is shaded in light grey, and highlights unmapped areas of the sea ice.

The Cryosphere Discuss., doi:10.5194/tc-2016-21, 2016
Manuscript under review for journal The Cryosphere
Published: 2 February 2016

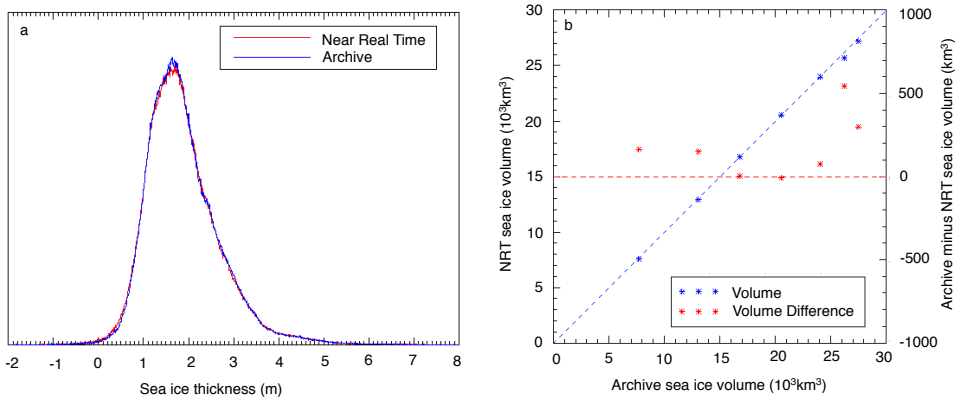

Figure 2: Comparison of near real time (NRT) and archive estimates of Arctic sea ice thickness and volume, from CryoSat-2. (a) Normalised distribution of NRT and archive thickness estimates over the period October 2014-April 2015, for all grid cells where measurements are available for both datasets. (b) Crossplot of sea ice volume for October 2014-April 2015. Also shown is the difference (archive minus NRT) in sea ice volume between the datasets.

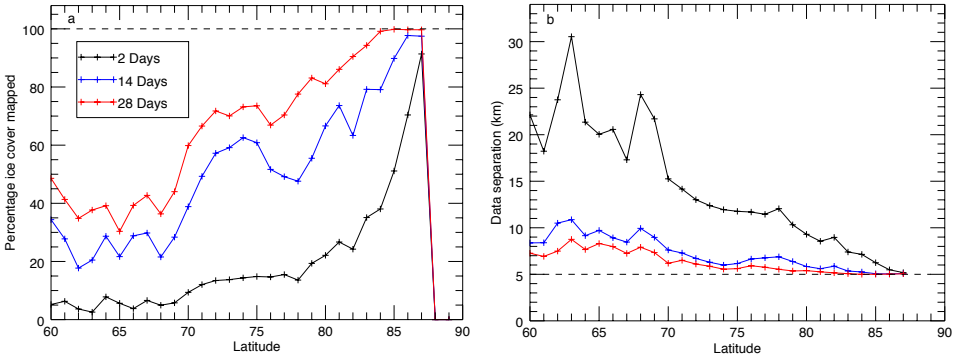

Figure 3: Spatial and temporal sampling of the Centre for Polar Observation and Modelling (CPOM) near real time (NRT) Arctic sea ice thickness product, north of 60°N. (a) Plot showing the percentage of sea ice cover mapped in 1° latitude bands, averaged over each month from October 2014-April 2015. Data are plotted for the final 28, 14, and 2 days of all months. (b) Plot showing the mean separation between NRT measurement points in 1° latitude bands, averaged over each month from October 2014-April 2015. Data are plotted for the final 28, 14, and 2 days of all months.

The Cryosphere Discuss., doi:10.5194/tc-2016-21, 2016
Manuscript under review for journal The Cryosphere
Published: 2 February 2016

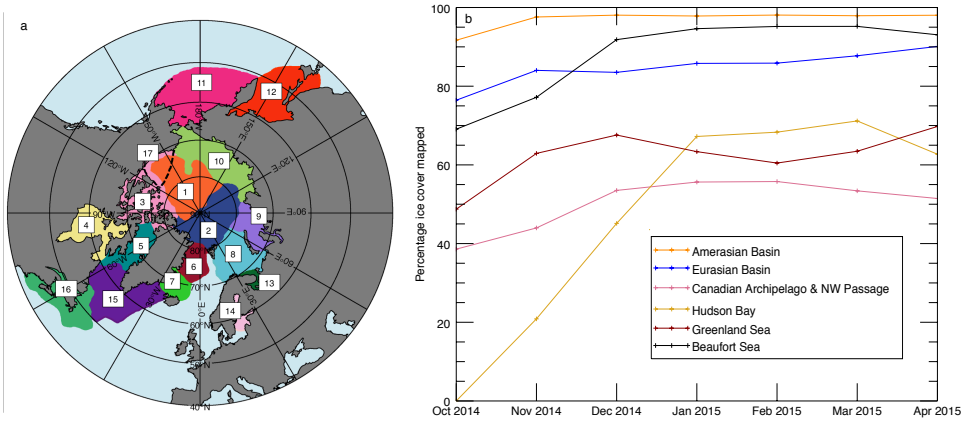

Figure 4: Regional and temporal sampling of the Centre for Polar Observation and Modelling (CPOM) near real time (NRT) Arctic sea ice thickness product. (a) Arctic Ocean regions selected for analysis. The regions are the Amerasian Basin (1), Eurasian Basin (2), Canadian Archipelago and Northwest Passage (3), Hudson Bay & Foxe Bay (4), Baffin Bay (5), Greenland Sea (6), Iceland Sea (7), Barents Sea (8), Kara Sea (9), Siberian Shelf Seas (10), Bering Sea (11), Sea of Okhotsk (12), White Sea (13), Baltic Sea & surrounding Gulfs (14), Labrador Sea (15), the Gulf of St Lawrence & Nova Scotia Peninsula (16), and the Beaufort Sea (17). Regions 1-10 encompass all autumn sea ice, and regions 1-16 encompass all spring sea ice. Region 17 is a sub-region of region 1 and 3. (b) Plot showing the percentage of sea ice cover mapped in each month, for six key oceanographic basins. This plot shows the data coverage for the final 28 days of each month. The basins are the Amerasian Basin, Eurasian Basin, Canadian Archipelago and Northwest Passage, Hudson Bay, Greenland Sea, and the Beaufort Sea.